Expanded View Figures

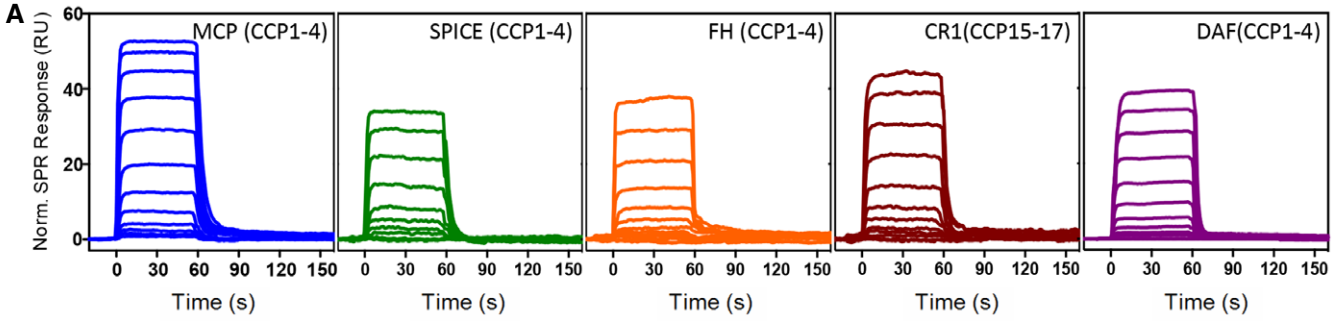

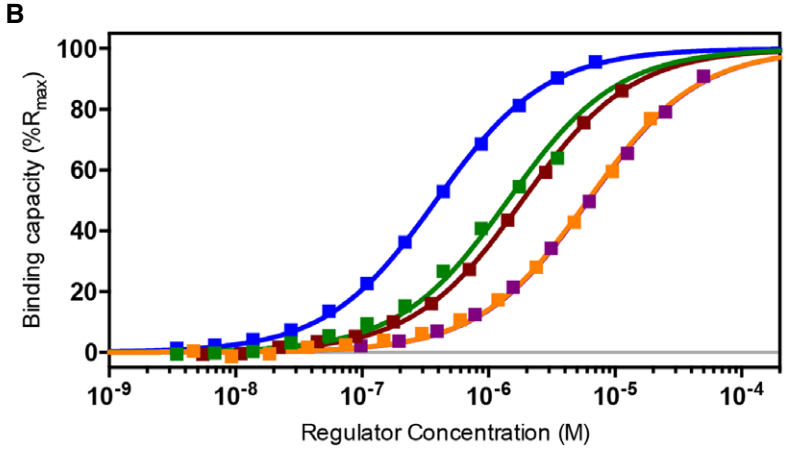

Regulator	K_D (μM)
MCP(CCP1-4)	0.35 ± 0.01
SPICE	1.31 ± 0.16
CR1(CCP15-17)	1.93 ± 0.12
FH(CCP1-4)	7.16 ± 0.24
DAF(CCP1-4)	6.08 ± 0.11

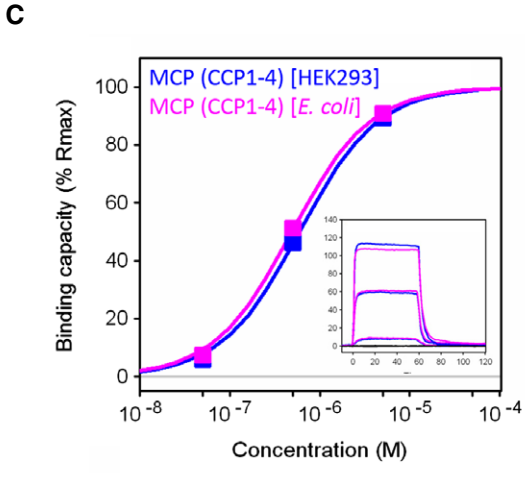

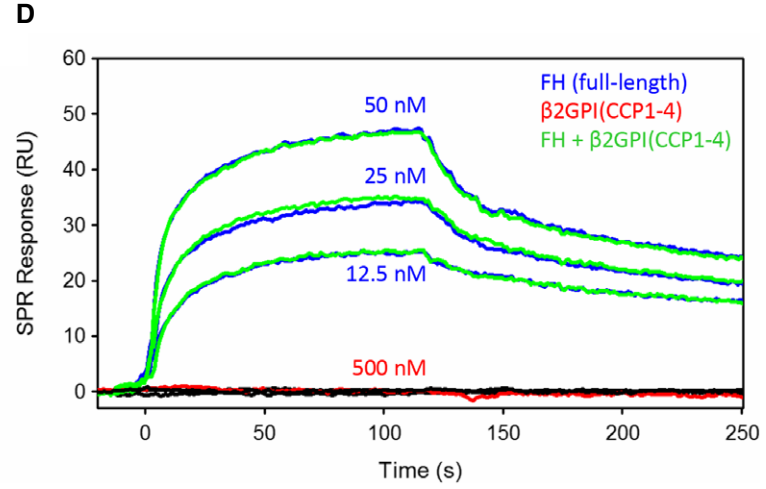

Figure EV1. Interaction of regulator proteins with C3b as determined by surface plasmon resonance.

A–C The C3b binding affinity of all regulators used in this study was measured by SPR on a surface that was prepared via on-chip convertase-mediated deposition of C3b. All regulators showed dose-dependent binding over the injected concentration ranges [MCP (CCP1–4) = 0.003–7 μM, SPICE = 0.003–3.5 μM, FH (CCP1–4) = 0.005–19 μM, CR1 (CCP15–17) = 0.005–11 μM, and DAF (CCP1–4) = 0.09–50 μM] with rapid dissociation phases that resulted in block-shaped response curves. Reported values for binding affinities (K_D) range from 0.5 to 10 μM (Liszewski *et al*, 2006; Harris *et al*, 2007; Wu *et al*, 2009), with the order of affinity MCP > SPICE > FH > CR1 > DAF (A). All SPR response curves were normalized for molecular weight of the regulator and surface density of C3b. The steady state responses of all regulators could be fitted to a single binding site model, resulting in the listed K_D values (B). Of note, DAF (CCP1–4) was evaluated in a separate experiment under the same conditions and superimposed with the normalized results of the other regulators. In the case of MCP, the *E. coli*- and HEK cell-produced protein essentially showed the same binding and affinity (C); only MCP from *E. coli* is shown in panels (A) and (B). Among the regulators, MCP (CCP1–4) showed the highest affinity to C3b with a K_D ~350 nM, slightly stronger than in recently published SPR data for the interaction of soluble MCP (CCP1–4) to randomly immobilized C3b (K_D ~1 μM; Heurich *et al*, 2011). Recombinant SPICE showed an affinity of 1.3 μM affinity to C3b**;** previous studies in low-salt buffer also indicated a stronger binding of MCP when compared with SPICE (Liszewski *et al*, 2006), yet the K_D difference observed here is smaller. CR1 (CCP15–17) bound with slightly weaker affinity (K_D ~2 μM) as SPICE. On the other hand, SPICE bound with higher affinity to C3b than recombinant DAF (CCP1–4) and FH (CCP1–4), which yielded K_D's of 6.1 and 7.2 μM, respectively. Similar to other studies (Morgan *et al*, 2011), physiological deposition of C3b appears to generate slightly stronger affinities when compared to the previously reported K_D of 11 μM for FH (CCP1–4) binding to non-enzymatically deposited C3b (Wu *et al*, 2009). Indeed, the affinity for DAF determined here is much closer to previous values of DAF binding to thioester-deposited C3b (K_D = 7 μM) when compared to randomly deposited C3b (K_D = 14 μM; Harris *et al*, 2005).

D The plasma protein β2-glycoprotein 1 (β2GPI) had previously been described to bind C3b via its CCP domains 1–4 and enhance the binding of FH to C3b (Gropp *et al*, 2011). When replicating the conditions of the previous ELISA-based study on SPR, no direct binding of β2GPI (CCP1–4) to C3b could be observed at a concentration of 500 nM. Similarly, no enhancement of FH binding (12.5–50 nM) was detected in the presence of 500 nM β2GPI (CCP1–4).

Figure EV2. Analysis of C3b-regulator interactions divided by contact site.

A Histograms showing the most prominent features of C3b-regulator interactions normalized for comparison among regulator structures. Shown are total number of amino-acid contacts, buried surface area, electrostatic, and hydrophobic contacts. The histogram bar colors refer to each regulator molecule as shown in Fig 1A. For each C3b contact site, the contribution of each interaction is provided as percentage from the total contact interface of the regulator.

B Specific details of C3b-regulators interaction sites. Each of the four panels, representing binding sites CCPi–iv as described Fig 2, shows the contact site between C3b (displayed as cartoon) and the surface contour of a regulator (FH) to highlight its steric hindrance. Amino acids of C3b involved in protein–protein interactions have their side chains shown as ball-and-sticks and labeled with residue numbering. The alignments above each panel show the amino acids of the various complement regulators involved in binding. Underlined residues are buried in the contact interface. Residues involved in specific hydrogen-bonding interactions, salt bridges, or strong hydrophobic contacts are highlighted with the color of the C3b domain corresponding to the specific interaction site. The limited resolution (4.2 Å) of the C3bDAF (CCP2–4) structure precludes a detailed interpretation of the contact interface. In this case, the sequence coloring refers to amino-acid proximity between DAF and C3b residues likely involved in hydrogen-bonding interactions.

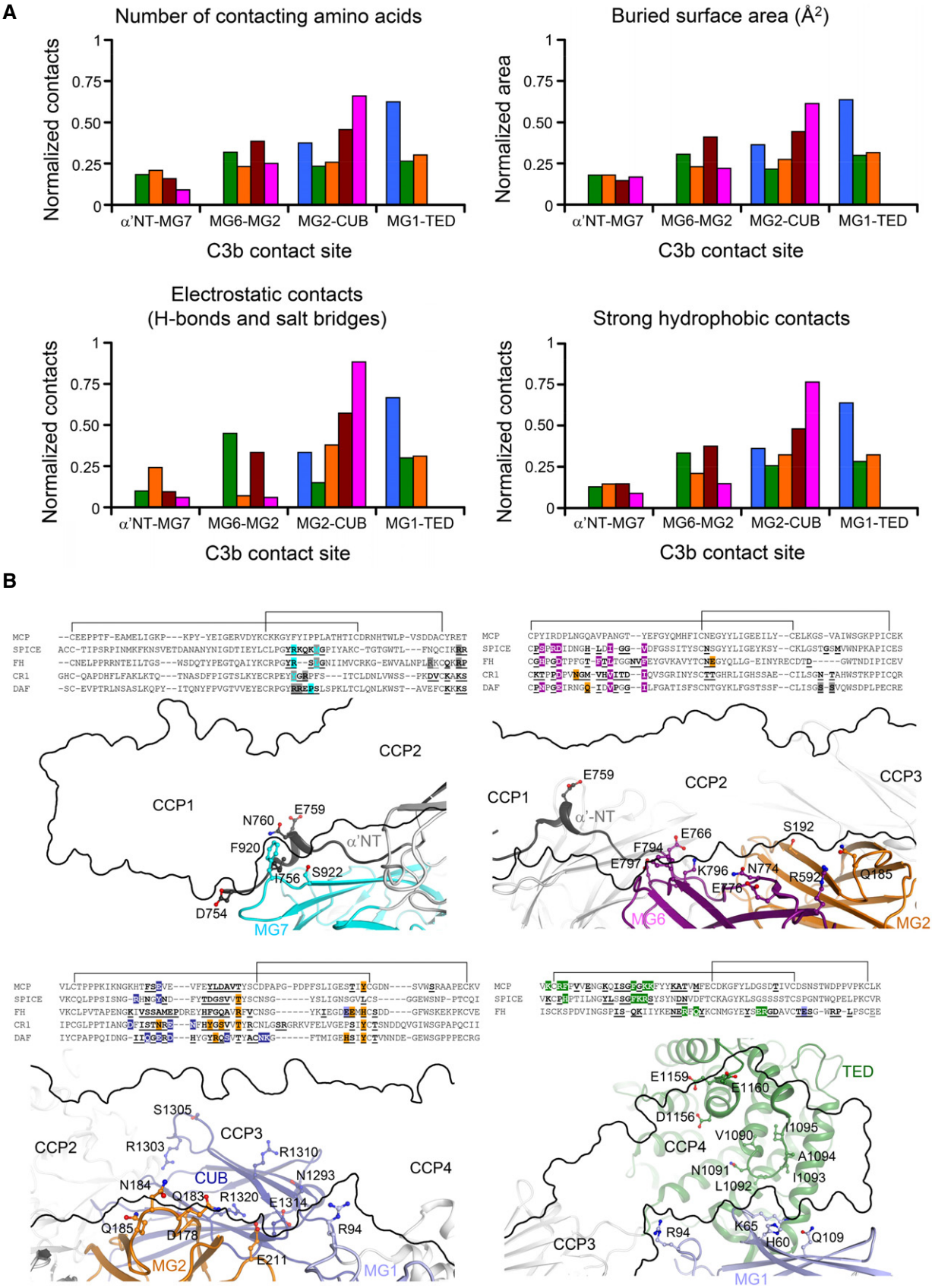
A
Number of contacting amino acids
Normalized contacts
1
0.75
0.50
0.25
0
α'NT-MG7
MG6-MG2
MG2-CUB
MG1-TED
C3b contact site
Buried surface area (Å2)
Normalized area
Electrostatic contacts
(H-bonds and salt bridges)
Strong hydrophobic contacts
B
MCP
SPICE
FH
CR1
DAF
CCP1
CCP2
CCP3
CCP4
α'-NT
MG7
MG6
MG2
MG1
CUB
TED
N760
E759
F920
I756
S922
D754
E766
S192
F794
E797
K796
N774
R592
Q185
E776
S1305
R1303
R1310
N1293
N184
Q183
R1320
E1314
Q185
D178
R94
E211
E1159
E1160
D1156
V1090
I1095
A1094
N1091
I1093
L1092
K65
H60
Q109

Figure EV2.

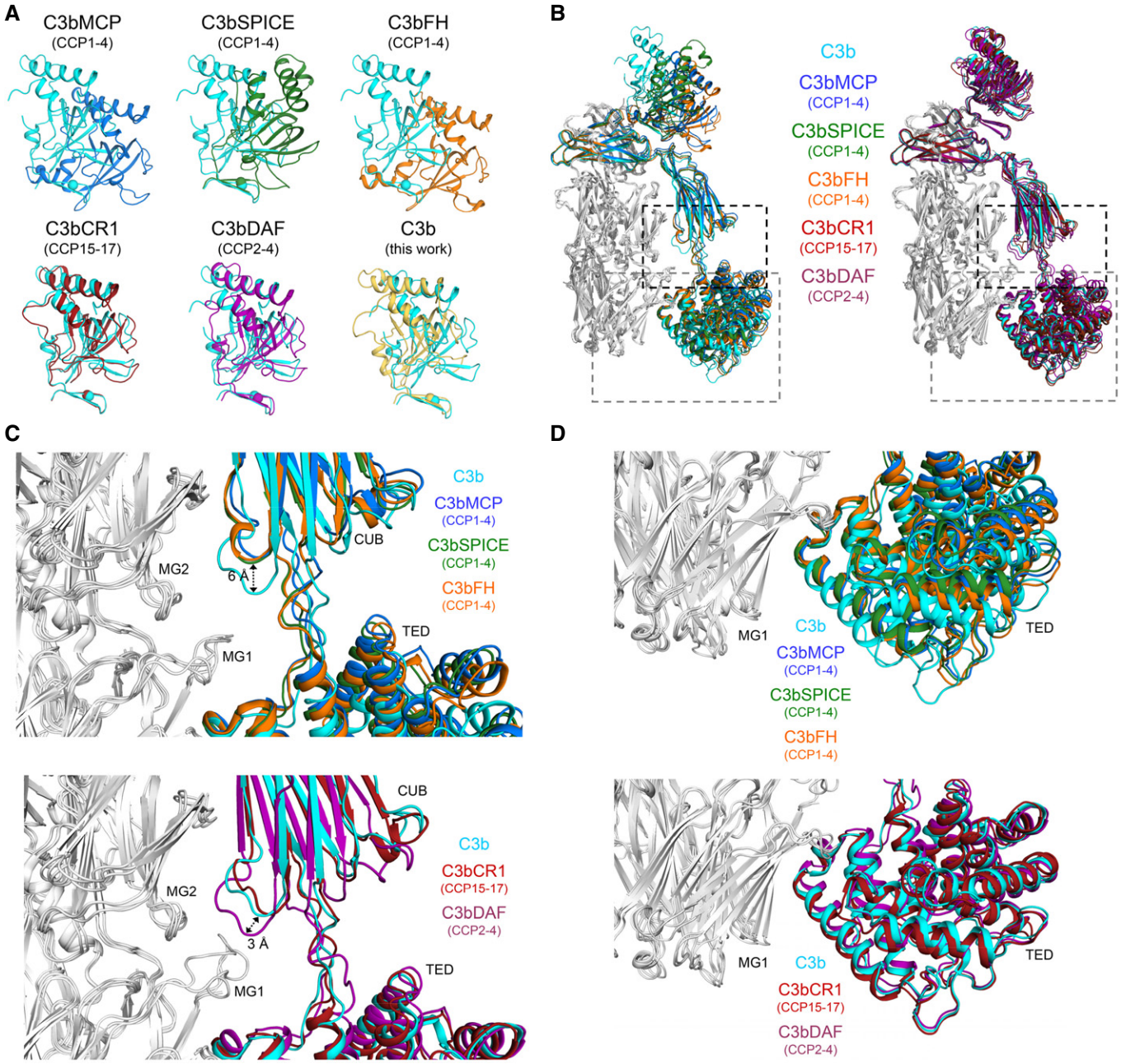

Figure EV3. Comparison of the observed structural features in C3b-regulator complexes with DAA and CA.

A Orientations of the CTC domains in the various C3b-regulator complexes, represented as cartoons. C3b from Janssen *et al* (2006) is used as reference (shown in cyan).

B Superposition of C3b structures from the C3b-regulator complexes showing upward (left) and downward (right) shifts of CUB-TED domains compared to free C3b (cyan).

C Details of the upward (top) and downward (bottom) CUB-TED shift around the CUB-TED linker region.

D Details of the upward (top) and downward (bottom) CUB-TED shift at the bottom of the TED domain.

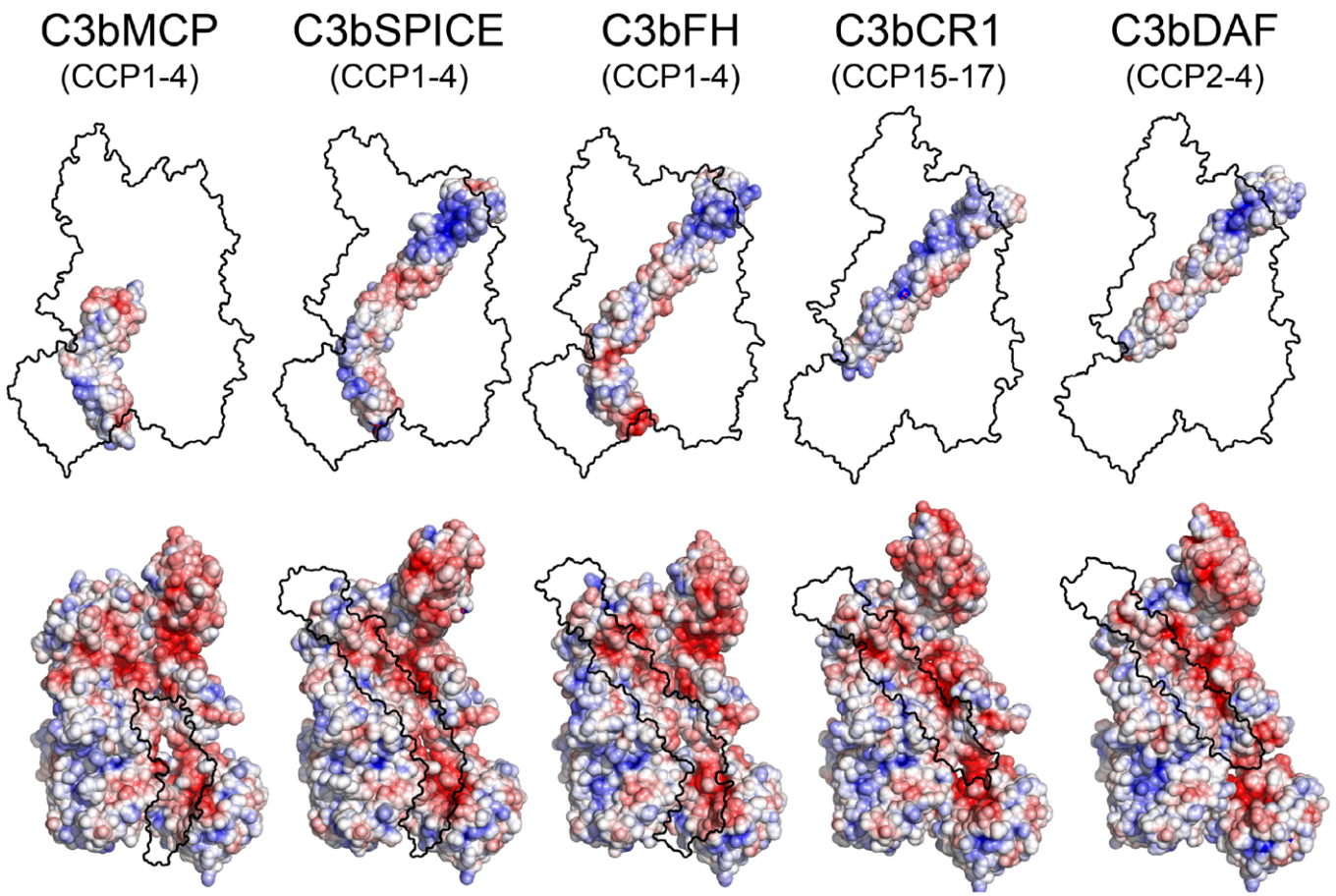

Figure EV4. Electrostatic interactions at the C3b-regulator interfaces.
Surface representations of separated regulators (top) and C3b (bottom) structures, colored based on their electrostatic potentials as computed using APBS (Baker *et al*, 2001) from $-5\ k_bTe_c^{-1}$ (red) to $+5\ k_bTe_c^{-1}$ (blue). The contact interface is shown on three-dimensional surface with a black contour drawing of the corresponding binding partner.

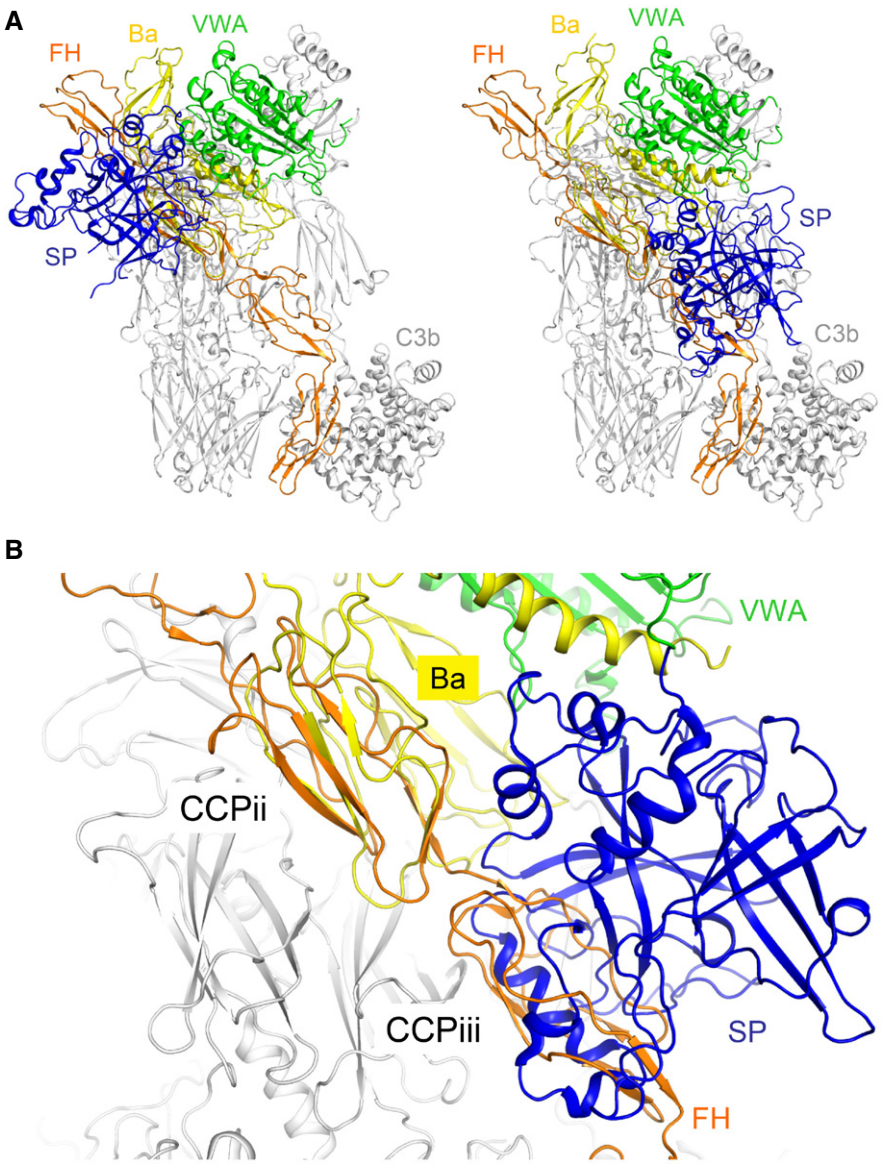

Figure EV5. Details of the overlapping binding site on C3b for regulators and FB.

A Cartoon representation of the superposition between C3b-FH (CCP1–4) and the C3b-FB complex in its closed (left, model based on the CVF-FB structure (Janssen *et al*, 2009)) and "open" (right) states (PDB ID 2XWJ; Forneris *et al*, 2010).

B Zoomed view of the superposition of C3b-FH (CCP1–4) with the "open" state of C3b-FB. The CCPii site shows complete overlap between FH CCP2 (orange) and FB CCP2 (yellow). In the "open" state of FB, the SP domain of the protease (blue) overlaps with the binding site for FH CCP3.